IEEE Access
Multidisciplinary ⋮ Rapid Review ⋮ Open Access Journal

Received June 16, 2020, accepted June 30, 2020, date of publication July 15, 2020, date of current version July 23, 2020.

Digital Object Identifier 10.1109/ACCESS.2020.3008253

Analysis and Treatment of an Overheated Ablated Fault on the Pole Shoe Surface of a Large Tubular Hydro-Generator

ZHI-TING ZHOU[1], YONG YANG[2], KE XIAO[3], ZHEN-NAN FAN[3], ZU-YING BIAN[3], KUN WEN[3], JING-CAN LI[1], AND BING YAO[3]

[1]State Key Laboratory of Power Transmission Equipment and System Security and New Technology, Chongqing University, Chongqing 400030, China
[2]Research and Test Center, Dongfang Electric Machinery Company Ltd., Deyang 618000, China
[3]Key Laboratory of Fluid and Power Machinery, Ministry of Education, Xihua University, Chengdu 610039, China

Corresponding author: Zhen-Nan Fan (fanzhennan@126.com)

This work was supported in part by the National Natural Sciences Fund Youth Fund of China under Grant 51607146 and Grant 61703345, in part by the Key Scientific Research Fund Project of Xihua University under Grant Z1520907 and Grant Z1520909, in part by the Key Research Fund Projects of Sichuan Provincial Education Department under Grant 16ZA0155 and Grant 16ZB0159, in part by the Sichuan Science and Technology Program under Grant 2018GZ0391, in part by the Chunhui Project Foundation of the Education Department of China under Grant Z2016144, in part by the Open Research Subject of Key Laboratory of Fluid and Power Machinery, Ministry of Education, Xihua University, Chengdu, China, under Grant SZJJ2015-027, and in part by Altair for FLUX software support.

ABSTRACT Aimed at a new kind of overheated ablated fault on the pole shoe surface of a large tubular hydro-generator, based on the real site characteristics of the fault with combination of a physical field analysis, this paper reveals the occurrence mechanism of such faults from operational conditions, generator structure, material characteristics, and so on. On the basis of the results, the fault treatment and the generator improvement strategy are proposed. In addition, the treatment method has been applied to a faulty generator, and it successfully eliminating the fault. The research is of great significance for restraining the loss and heat of poles in large tubular hydro-generators as well as improving the safety and reliability of the operation of generators and power grids.

INDEX TERMS Analysis and treatment, overheated ablated fault, pole shoe surface, tubular hydro-generator.

I. INTRODUCTION

Since the development of middle and high hydraulic head hydro resources has been nearly completed, the development of low hydraulic head hydro resources is beginning to receive more attention. Compared to hydro-generators with medium and high water heads, which use impulse-type, mixed-flow-type, and axial-flow-type hydraulic turbine, the tubular hydro-generator is the best model for developing and utilizing low hydraulic head rivers and tidal energy resources, saving 20-30% of construction costs and increasing power generation by 3-5% [1]. However, the stator and rotor diameters and the air gaps in tubular hydro-generators are significantly smaller than those of other hydro-generators due to the large number of poles and the restrictions due to the hydraulic performance of flow channels and bulb bodies, resulting in a narrow and slender internal space, with the number of slots per pole per phase of $q \leq 2$ and the large tooth harmonic. Under these conditions, the difficulties in the design and manufacturing process significantly increase, and even a little negligence can lead to a series of problems, such as overheating and damage of the generator's magnetic pole components and deterioration of the no-load voltage waveforms.

Especially, in recent years, because of some improper designs, some large tubular hydro-generators have been frequently suffering from a new kind of overheated and ablated failures on the surface of their pole shoes when operated in a rated symmetry load condition, which not only seriously threatens the safe and stable operation of generators and power grids, but also causes huge economic losses and adverse social impacts on enterprises. In fact, according to the investigation of generator manufacturers, once such a fault occurs, it usually takes at least three months to repair the

The associate editor coordinating the review of this manuscript and approving it for publication was Wei Xu.

TABLE 1. The basic parameters of generator.

Parameter	Value
Rated power (MW)	34
Rated voltage (V)	10.5
Rated current(A)	1968
Power factor	0.95
Number of magnetic poles	44
Number of slots per pole per phase	2
Stator slot skewed degree(t_1)	1

generator. No matter the cost of generator maintenance or the loss of power generation revenue during maintenance, it is undoubtedly great. Therefore, in order to solve above problems, it is necessary to perform a comprehensive, in-depth, and effective research on the occurrence mechanisms and treatment measures of this new type of failure.

To date, although in area of the rotor loss and heat of hydro-generator, researchers have carried out some constructive study and made a number of significant achievements [2]–[16], including the analytical calculation and numerical analysis of damper winding current and loss [2]–[4], the electromagnetic-temperature field coupling analysis of damper winding loss and heat [5]–[7], the discussion of the influence of structural parameters on damper winding loss and heat [8], [9],and the coupling analysis of fluid- temperature field of rotor pole heat [10]–[16]. However, none of above research work involves the analysis of the overheat fault of the hydro-generator rotor. In particular, it should be noted that up to now, few related research work has been published for this newly discovered overheated ablated fault of the pole shoe surface of tubular hydro-generator. Therefore, in order to avoid the huge economic loss caused by this kind of fault and improve the safety of generator and grid operation, it is necessary to study its occurrence mechanism and treatment measures.

In this study, we take a real 34MW tubular hydro-generator with such kind of fault as an example (the basic parameters are shown in Table 1). Then, based on the characteristics of the fault generator, a variety of research methods were used, such as power plant operation analysis, a lamination simulation heat test, a lamination material test, and physical field calculation. On the basis of all these works, we comprehensively, systematically, and accurately reveal the mechanism of the fault. Moreover, an optimal design measure and an improvement method of the fault generator were put forward, which were also used to repair the faulty generator. The site test results showed that the improvement method was effective and that the fault was completely eliminated.

In the Table 1,t_1 is the stator slot pitch.

II. FAULT CHARACTERISTICS

The hydro-generator was officially put into operation on May 28, 2006, and a serious overheated ablated fault on the surface of its pole shoe was found during the first overhaul in January 2014. After disassembling the magnetic poles, it was found that this kind of fault has the following characteristics,

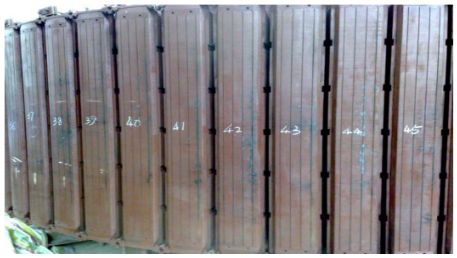

(a)Overheated ablated magnetic poles(a faulty generator)

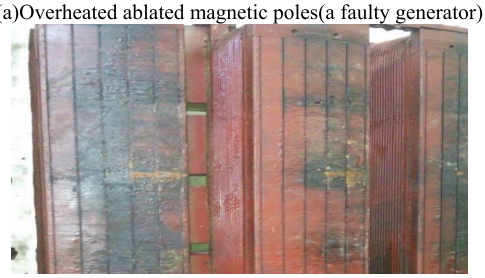

(b)Overheated ablated magnetic poles(a faulty generator in another hydropower station)

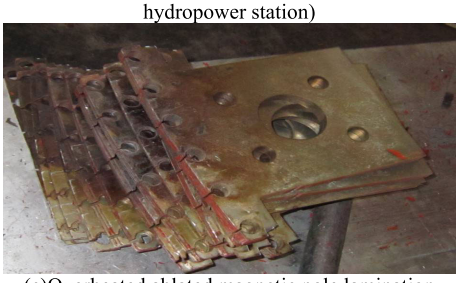

(c)Overheated ablated magnetic pole lamination

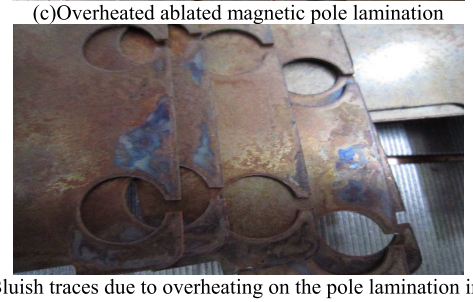

(d)Bluish traces due to overheating on the pole lamination in the downstream region

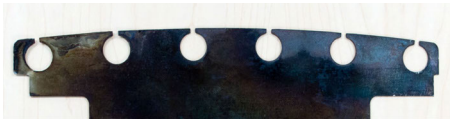

(e)Bluish traces due to overheating on the pole lamination in the upstream region

FIGURE 1. Overheated ablated pole lamination after pole disassembly.

as shown in Fig. 1, which were rarely noted in former hydro-generators.

First, the overheated traces are distributed in the shallow surface area of the pole shoe core, and the overheating propagation direction is from the surface of the pole shoe core to its interior.

Second, the surface area of the pole shoe core is seriously overheated and ablated, even looking bluish because of overheating.

Third, there is an uneven distribution of the overheated area, which is mainly distributed in the leeward area of the

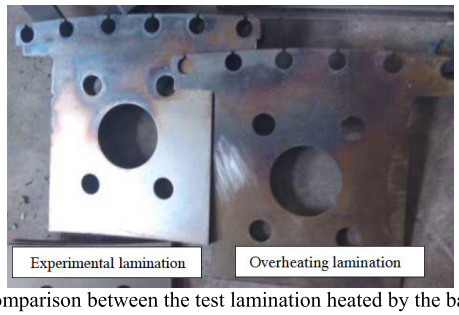

(a)The comparison between the test lamination heated by the baking gun and the lamination with overheating fault

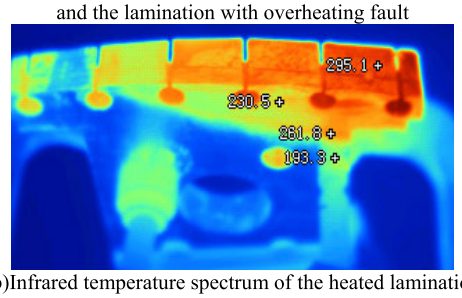

(b)Infrared temperature spectrum of the heated lamination

FIGURE 2. Simulation test of the overheated fault temperature by heating the pole lamination with the baking gun.

pole shoe iron core. Moreover, the overheated area in the upstream area is more serious than that in the downstream area.

Fourth, overheating only occurred in the shallow surface area of the pole shoe core, and there are no traces of overheating on the damper bar.

III. FAULT TEMPERATURE SIMULATION TEST

To determine the temperature condition in the overheated area of the pole shoe under the fault condition, a simulated heating test was performed on the normal iron core lamination, and discoloration of the lamination after heating was observed. The temperature of the lamination under the overheated fault condition was concluded by comparing it with that of the lamination that had an overheated fault. Specifically, the following two simulated heating test measures were taken.

First, we heated the surface of the pole shoe with the open fire of a baking gun, simulated the high temperature and heat transfer process of the pole shoe surface,and observed the discoloration of the paint film and the lamination.Then, we used a thermocouple and an infrared thermal imager to measure the temperature of the overheated position. The measurement results showed that the highest temperature at the overheated position was not lower than 295 °C, as shown in Fig. 2.

Second, we placed the pole lamination in the oven, adjusted the oven temperature from 180 °C to 300 °C, took out 3 laminations in turn every 10 °C temperature rise, and kept each lamination temperature for 4 hours. Finally, it is found that the maximum temperature should be at least 290 °C if the pole lamination is overheated to be bluish, as shown in Fig. 3.

On the basis of the above test results, it can be considered that the maximum temperature in the fault area shall not be lower than 290 °C when the pole shoe fault occurs.

FIGURE 3. Bluish mark is shown on the pole lamination when heated to 290 °C in the oven.

IV. SPECULATION ON POSSIBLE CAUSES OF THE FAULT

The results of disassembling the faulty pole show that there is no sign of overheating in the damper winding. Therefore, the possibility that the fault is caused by the heat of the damper winding is eliminated. In addition, on the basis of the above fault phenomena and the temperature simulation test results, it is preliminarily concluded that the possible fault causes could be as follows:

First, there may be an unbalanced load in the power system, which leads to an excessive negative sequence current of the generator, causing a negative sequence magnetic field that induces a large eddy current loss and extra heat on the surface of the pole shoe.

Second, the harmonic magnetic fields, such as the generator tooth harmonic, the power system harmonics, and the excitation power source harmonic, may have higher values, which induces a large eddy current loss and extra heat on the surface of the pole shoe.

Third, through the site investigation, it was found that tubular hydro-generators with this kind of fault adopt a stator slot skewed structure. However, other generators without this structure did not have such faults. Therefore, it is speculated that the stator slot skewed structure may not be suitable for tubular hydro-generators or that in tubular hydro-generators, due to the use of stator slot skewed structures, an excessive eddy current loss and extra heat surface are brought about on the surface of the pole shoe.

Therefore, these three possibilities are analyzed to find out the cause of this failure.

V. ANALYSIS OF NEGATIVE SEQUENCE CURRENT INFLUENCE

The statistics of the negative sequence current limit protection alarms during 2009-2013 in the power plant in which the faulty generator was located is detailed in Table 2. Its negative sequence setting limit is 12.6% (close to 12% of the value specified in the Chinese national standard).

Based on the operation data mentioned above, it can be seen that the longest negative sequence current duration of this generator was 1.357s, which occurred on August 2, 2010. Therefore, it can be considered that the generator did not run asymmetrically for a long time and that it should be analyzed according to the requirements of the transient negative sequence capacity.

According to the requirements of the Chinese national standard (GB/T 1029-2005) on the operation capacity of

TABLE 2. Statistics of negative sequence current over limit protection of fault generator in 2009-2013.

Start time	Maximum negative sequence current in the recorded waveform(Secondary side actual value)/A	Duration (ms)	Possible causes of negative sequence current
2009. 9. 10. 03. 46. 27	0.462	61	system impact
2009. 9. 10. 05. 57. 42	0.251	210	system impact
2010. 8. 02. 03. 13. 25	0.526	1357	system impact

TABLE 3. Statistics of generator negative sequence capability.

Negative sequence overrun time	I_2 (Secondary side actual value)/A	I_2/I_N (per unit/p. u.)	t /s	$(I_2/I_N)^2$t /s
2009. 9. 10	0.462	0.58212	0.061	0.021
2009. 9. 10	0.251	0.31626	0.21	0.021
2010. 8. 2	0.526	0.66276	1.357	0.596

air-cooled hydro-generators under short-term asymmetric loads, the capacity of the transient negative sequence is calculated based on $(I_2/I_N)^2$t, and the results are provided in Table 3.

The results show that, although the negative sequence current keeps the maximum value during the continuous recording process, the maximum value of $(I_2/I_N)^2$t does not exceed 0.6s, which is considerably less than the 40s of the Chinese national standard.

Thus, on the basis of all these data, it can be concluded that the negative sequence current is not the main cause of this kind of fault.

VI. HARMONIC IMPACT ANALYSIS

A. THE INFLUENCE FROM THE TOOTH HARMONIC OF THE AIR GAP MAGNETIC FIELD

According to the design theory of the hydro-generator, the ordinal number of the tooth harmonic is given as follows [17], [18]:

$$\nu = k2mq \pm 1 \tag{1}$$

where k is the order of the tooth harmonic, m is the number of phases, and q is the number of the slots per pole per phase. For this generator, $m = 3$, $q = 2$, and the first-and second-order tooth harmonics are (11, 13) and (23, 25), respectively.

It should be noted that, for a tubular hydro-generator with a compact structure and a low rotation speed, in the selection of the electromagnetic design scheme, the number of slots per pole per phase is relatively small. Especially, for the integer slot design scheme with q=1 or 2, the first-order tooth

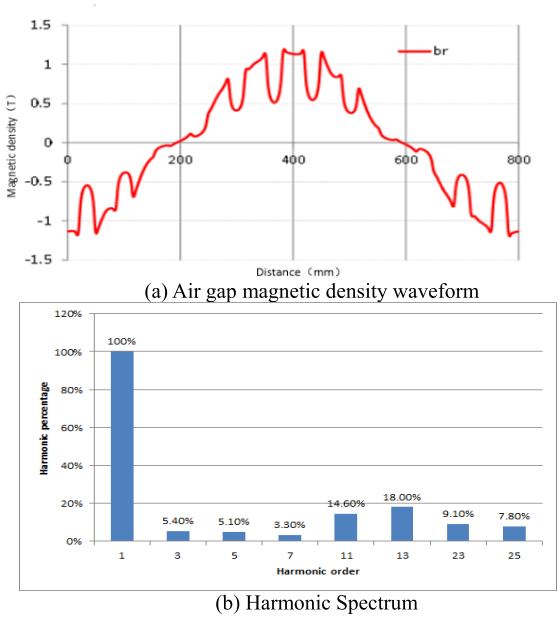

(a) Air gap magnetic density waveform

(b) Harmonic Spectrum

FIGURE 4. The air gap magnetic density waveform and harmonic spectrum of the faulty generator.

harmonic content is usually considerably large. So, to reduce the tooth harmonic potential in the no-load voltage, a stator slot skewed structure or an asymmetric damper winding is typically adopted. This is the inherent difficulty in the design of tubular hydro-generators.

Therefore, we obtain the tooth harmonic distribution of this faulty hydro-generator through the FEM calculation of the electromagnetic field, which is shown in Fig. 4.

The results of the above calculation show that the tooth harmonic content of the air gap magnetic field of the faulty generator is relatively high. However, according to our experience of generator design and manufacturing, we find that most of the tubular hydro-generators have this problem, but, not all tubular hydro-generators have such a serious overheating phenomenon on the surface of their pole shoe. Therefore, it can be concluded that the high harmonic content of the air gap magnetic field is not the primary reason for such faults.

B. INFLUENCE OF POWER SYSTEM HARMONICS

The power plant in which the faulty hydro-generator was located has made statistics on the terminal voltage harmonics of the faulty generator from 2009-2013, as shown in Table 4.

By comparing Table 4 with Table 2, it can be seen that when the terminal voltage harmonics are relatively high, the negative sequence current becomes significant. That is, for this faulty generator, the terminal voltage harmonics are usually nonexistent (or remarkably small). Even when the occasional organic terminal voltage harmonics are relatively high, it is because of short-term asymmetric loads that result in additional effects. Therefore, it can be concluded that the power system harmonics are not the primary reason for this type of fault.

TABLE 4. Statistics of the terminal voltage harmonics of the faulty generator from 2009-2013.

Start Time	phase	Maximum harmonic content of terminal voltage		
		Fundamental	Secondary	Third
2009. 9. 10. 03. 46. 27	Ua	58.6V	0.29%	3.01%
	Ub	53.1V	8.84%	2.90%
	Uc	53.3V	9.63%	2.50%
2009. 9. 10. 05. 57. 42	Ua	56.4V	4.19%	1.64%
	Ub	56.5V	4.41%	1.78%
	Uc	59.0V	0.17%	2.52%
2010. 8. 02. 03. 13. 25	Ua	53.4V	11.0%	2.80%
	Ub	57.2V	0.23%	2.00%
	Uc	53.8V	10.7%	0.75%

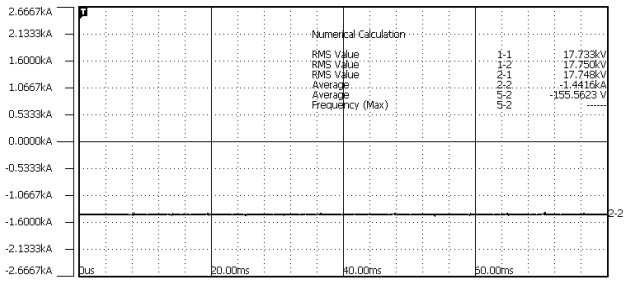

FIGURE 5. Oscillogram of the excitation current.

C. INFLUENCE OF THE EXCITATION POWER SOURCE HARMONIC

In the SCR excitation system, the excitation voltage has a high harmonic frequency of 300 Hz. However, due to the strong role of the rotor inductance, it can be regarded as a low-pass filter, where most of the harmonics are filtered out. Thus, basically, the excitation current will only have DC components, and there will not be any obvious harmonic components, not to mention cause such serious faults. This can be confirmed in the recorded spectrum of the excitation current. Fig. 5 is an oscillogram of an excitation current of a generator in a power station.

In addition, even if we step back to assume that the pole heating is caused by the excitation current harmonic, the pole's magnetic field will have the same change. That is, the loss and heat of pole will be uniform and not concentrated only on the pole shoe surface.

Therefore, it can be assumed that the excitation power source harmonic is not the primary reason for this kind of fault.

VII. ANALYSIS OF THE INFLUENCE OF THE STATOR SLOT SKEWED STRUCTURE

To date, most of the research work on the slot skew structure had focused on improving the voltage waveform, weakening the ripple torque of the slot, improving the operational stability, and so on. However, there were few studies on the shortcomings of this structure. In particular, we need to pay attention to the fact that in the investigation site of this fault, we found out that the generators that had adopted the stator slot skewed structure had this fault, whereas other generators did not. Therefore, we speculate that the stator slot skewed structure is likely the main cause of this kind of fault.

We used the electromagnetic field theory of electrical machinery to explain the reason for this conclusion, as follows:

When the stator slot skewed structure is adopted, although the fundamental wave magnetic density produced by the excitation winding is in the same phase in the axial direction, but the armature reaction fundamental wave magnetic density produced by the stator magnetic potential is shifted a pitch from one end to the other end of the generator such that the amplitude of the resulting air gap magnetic density is different from one end compared to the other. At the same time, all the harmonics, including those caused by the interaction of the tooth permeance with the harmonic magnetomotive force, have a similar phasor synthesis relationship. For example, the amplitude of the air gap flux density harmonics caused by the stator slotting under a load condition is higher at one end of the generator that at the other end.

In addition, the calculation results of the generator's magnetic field distribution also confirm this point, which is, when the stator slot skewed structure is adopted, the magnetic density of the rotor increases along the axial direction. Moreover, not only the magnetic density at the upstream end is significantly larger than that at the downstream end but also the area of the high magnetic density at the upstream end is significantly larger than that at the downstream end, as shown in Fig. 6.

This condition causes the following consequences:

First, the iron loss of the pole shoe is larger than that in the case of the stator slot no skewed structure. Second, it will increase this iron loss along the axial length of the pole. Thus, the heat of the pole shoe surface at the upstream end is significantly more than that at the downstream end. This resulted in the following failure phenomena:the overheating traces are distributed in the shallow area of the pole shoe core. And the overheating in the upstream area is significantly more than that in the downstream area.

From the above analysis, it can be concluded that the stator slot skewed structure should be the main cause of the fault.

VIII. IMPROVEMENT SCHEME ANALYSIS

Although from the above analysis, we could confirm that the stator slot skewed structure leads to an excessive iron loss from the pole shoes, which is the main reason for this kind of fault.But at the same time, we noticed that the main purpose of the stator slot skewed structure is to optimize the no-load voltage waveform and the grid-connected power quality. Therefore, while considering the elimination of such faults, it was necessary to ensure the no-load voltage waveform quality of the generator would still meet the following Chinese National Standard GB/T 1029-2005 [17].

One is the deviation of the actual waveform from the sinusoidal waveforms of the line voltage, and it is defined by

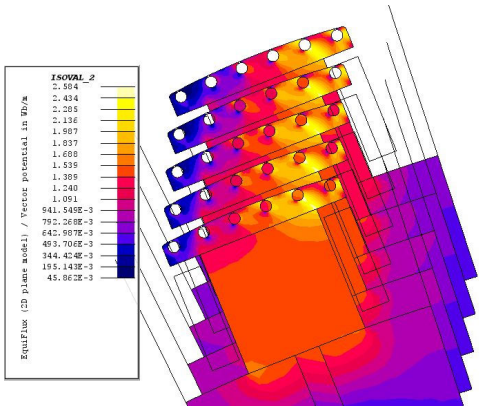

(a)The magnetic density of the rotor increases along the axial direction

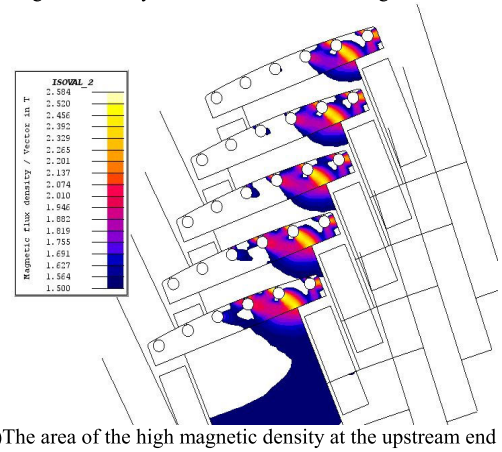

(b)The area of the high magnetic density at the upstream end is significantly larger than that at the downstream end

FIGURE 6. Magnetic density of the pole increases along the axial direction due to the stator slot skewed structure.

the harmonic distortion factor (*HDF*):

$$HDF = \frac{\sqrt{U_2^2 + U_3^2 + \cdots\cdots + U_n^2}}{U_1} \times 100\% \qquad (2)$$

Second is the telephone harmonic factor (*THF*), which quantifies the disturbance of the voltage waveform harmonics in telecommunications,

$$THF = \frac{\sqrt{U_1^2\lambda_1^2 + U_2^2\lambda_2^2 + ... + U_n^2\lambda_n^2}}{U} \times 100\% \qquad (3)$$

where U is the actual line voltage, U_i (i = 1, 2, 3 ...n, n is the highest considered order) is the line voltage of the *kth* harmonic, and λ_k is the weighted coefficient of the *kth* harmonic.

For large generators, the above Chinese national standard GB/T 1029-2005 stipulates that *HDF* be ≤5% and that *THF* be ≤1. 5%.

Therefore, we must eliminate the series of faults on the premise while considering the no-load voltage waveform quality of the faulty generator when applying any maintenance or transformation schemes.

At the same time, we must also consider that once the stator slot skewed structure is canceled, the stator of the whole generator has to be rebuilt, and the cost and time will be unbearable for the power plant. Therefore, to retain the stator slot skewed structure, we developed the following two improvement schemes for the magnetic pole structure, as detailed in Table 5. The first scheme is the structure of shifting the pole shoe and damper winding centerline at the same time, as shown in Fig. 7, and in this scheme, t_1 is the stator slot pitch.

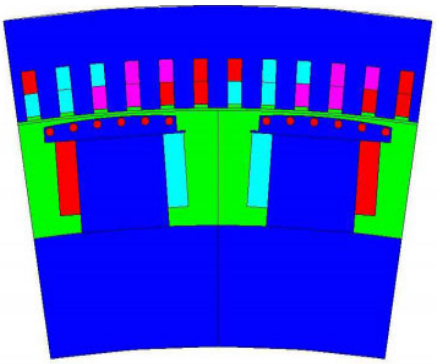

FIGURE 7. Scheme 1 in Table 5.

TABLE 5. Two improvement schemes.

Scheme number	Scheme content
1	Reserve the stator slot skew structure, rotor pole shoe, and damper winding center line shift 0.25 t_1 at the same time
2	Reserve the stator slot skew structure, reduce the thickness of the rotor pole steel lamination from 1 mm to 0.5 mm

TABLE 6. No-load volotage waveform quality parameters of the fault scheme and two improvement schemes.

Scheme number	HDF	THF
0 (failure scheme)	0.546%	0.526%
1	0.435%	0.283%
2	0.546%	0.526%

Through electromagnetic field analysis, the quality parameters of the no-load voltage waveform corresponding to the different types of improvement schemes are shown in Table 6. Under the rated symmetrical operating condition, the core loss of the pole shoe is shown in Table 7, and the damper winding loss is shown in Table 8. It should also be noted that, according to the requirements of the power plant and the manufacturer of the faulty generator, the per-unit value is adopted in Tables 7 and 8, where the base value is the relevant value of scheme 0 (i.e. the fault scheme).

It can be seen from the above results that, in the first scheme, although the no-load voltage waveform has been further optimized, the pole shoe core loss and the damper winding loss are not well restrained but increased by more than 10%. This obviously cannot eliminate the fault, which is not desirable.

TABLE 7. Pole shoe core losses of different schemes (rated symmetrical operation conditions).

Scheme number	Pole shoe core loss (per unit value)	
	Left magnetic pole	Right magnetic pole
0(failure scheme)	1	1
1	1.15	1.10
2	0.29	0.29

TABLE 8. Damper winding losses for different schemes (rated symmetrical operation conditions).

Scheme number	Damper winding loss (per unit value)	
	Left magnetic pole	Right magnetic pole
0(failure scheme)	1	1
1	1.14	1.10
2	1	1

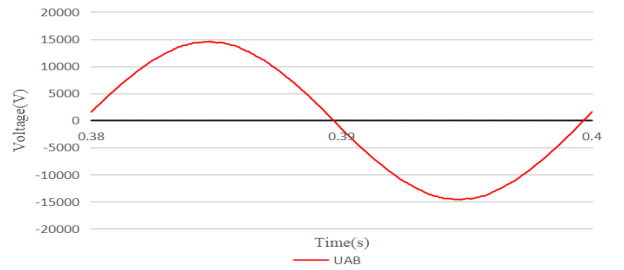

(a) Scheme 0

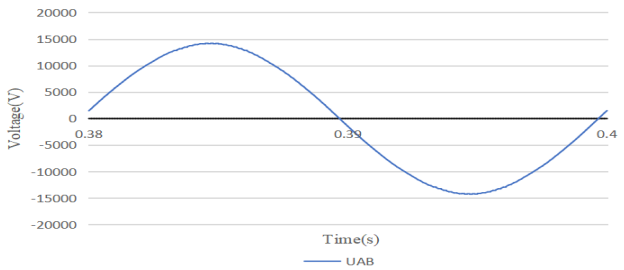

(b) Scheme1

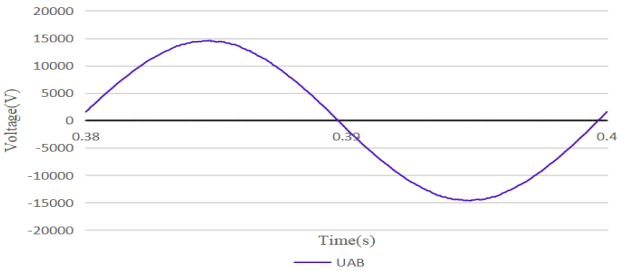

(c) scheme2

FIGURE 8. Comparison of the no-load voltage waveforms of different schemes.

In the second scheme, not only the no-load voltage waveform is of high quality but also the core loss of the pole shoe is significantly suppressed, which is only 29% of that of scheme 0 (i.e. failure scheme). In addition, and the damper winding loss does not increase with respect to scheme 0. Therefore, this scheme will significantly reduce the heat in the pole shoe area.

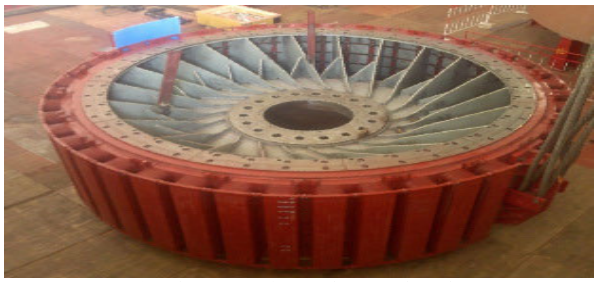

(a) The remanufactured magnetic pole

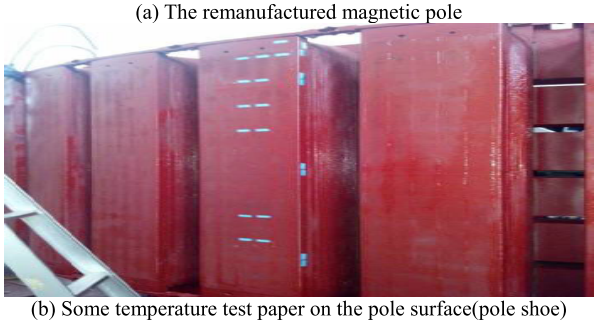

(b) Some temperature test paper on the pole surface(pole shoe)

(c) Some temperature test paper on the pole surface(pole end region)

FIGURE 9. Remanufactured magnetic pole and some temperature test paper on its surface (The new magnetic pole is made according to the second scheme).

The reason is that, in the aspect of the no-load voltage waveform optimization, for the generator whose number of slots per pole per phase is an integer, and when the structure of the stator slot skewed or the pole shoe and damper winding centerline shifting by $0.25t_1$ is separately adopted, the tooth harmonic of the no-load voltage can be weakened and the no-load voltage waveform can be optimized. However, if the above two structures are used at the same time, it is possible to make the effect of the waveform optimization more obvious, which is shown in Fig. 8. Therefore, the above two schemes can achieve a great no-load voltage waveform quality.

However, it should be noted that, in the above two schemes, the stator slot skewed structure was retained so the magnetic density and the core loss of the rotor pole can still increase along the axial direction. Therefore, other measures must be taken to effectively suppress the loss and overheating of the pole shoe core. In the second scheme, the use of thinner pole iron core laminations, which is equivalent to effectively increasing the resistance relative to the internal eddy currents of the pole iron core, can effectively inhibit the loss and overheating of the pole shoe iron core.

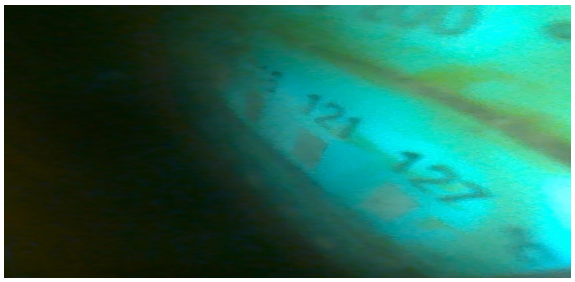

(a) The discoloration of the test paper at some positions observed by the endoscope

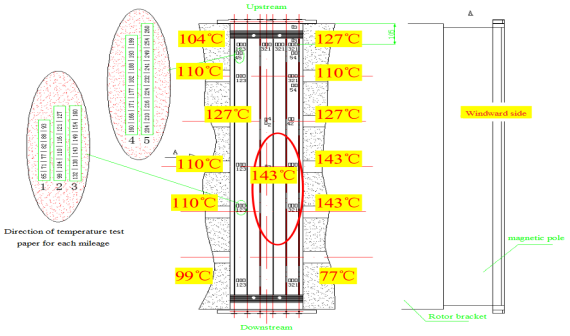

(b) Temperature distribution test results of pole 10

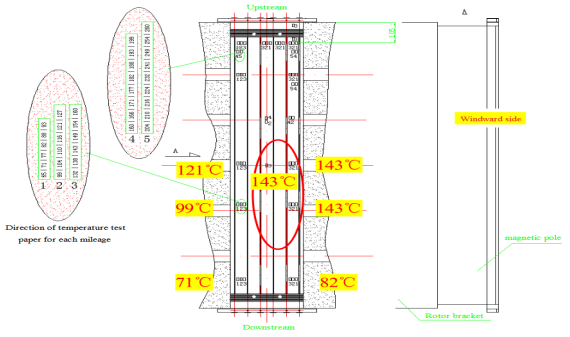

(c) Temperature distribution test results of pole 12

FIGURE 10. Test paper temperature measurement results of the pole shoe after the improvement.

IX. IMPROVEMENT PRACTICE AND EFFECT

On the basis of the above analysis results, we decided to implement the above-mentioned second scheme to repair the faulty generator. To test whether this scheme can effectively eliminate the overheating ablation fault of the pole shoe iron core, we arranged the temperature measurement test paper at some positions on the surface of the remanufactured pole shoe, as shown in Fig. 9.

From June 2016 (completion of improvement) to October 2016, the generator was symmetrically operated at full load for 100 days. Then, it was stopped, and the rotor was lifted out. The discoloration of the temperature measuring test paper on the surface of the pole shoe showed no signs of overheating or ablation. The relevant basic operation parameters are detailed in Table 9, and the relevant temperature measurement results are shown in Fig.10.

According to the above-mentioned chart data, it can be seen that the implementation of the second improvement scheme effectively eliminated the faults, as the maximum temperature of the pole shoe surface dropped from 295 °C (before the improvement) to 143 °C, with a decrease of 52%.

TABLE 9. Basic parameters of the generatorat full load after maintenance.

Parameter	Value
Rated power (MW)	32.6
Rated voltage (V)	10.42
Rated current(A)	1899
Excitation voltage(V)	205
Excitation current(A)	916
Cold air temperature(°C)	26.2
Hot air temperature(°C)	44.0

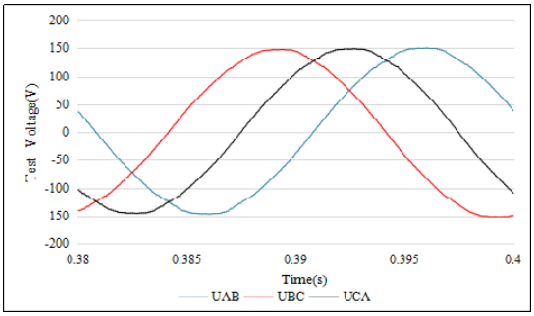

FIGURE 11. No-load voltage measurement waveform of the repaired generator.

TABLE 10. No-load voltage waveform quality parameters of the repaired generator.

Scheme 3	Harmonic percentage (%)					Waveform quality	
	1	11	13	23	25	*HDF* (%)	*THF* (%)
Calculated value	100	0.167	0.094	0.008	0.014	0.546	0.526

At the same time, before the generator was connected to the grid, we also measured the no-load voltage waveform, as shown in Fig. 11. The relevant waveform quality parameters are provided in Table 10, and they show that the no-load voltage waveform quality is considerably good.

On the basis of the above facts, we can conclude that this repair scheme is successful.

X. CONCLUSION

In this paper, we studied a new kind of an overheated ablated fault on the pole shoe surface of the tubular hydro-generator. On the basis of characteristics of the real site, several methods, such as temperature simulation tests, recording result analyses, and physical field calculations, were performed comprehensively to find out the mechanism of occurrence of a fault. Then, an improvement scheme was proposed and put into practice, and it achieved satisfactory results. The following important conclusions were then drawn:

1) The stator's slot skewed structure leads to a significant, uneven distribution of the magnetic density of the pole core along the axial direction, resulting in the core loss of the pole shoe that is much higher than other stators without slot

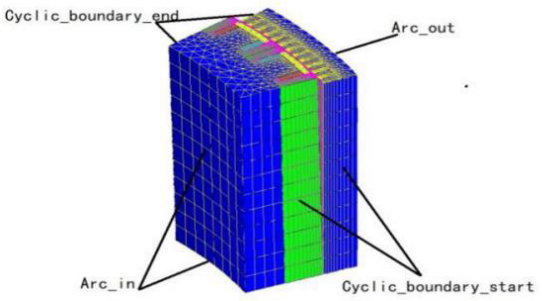

FIGURE 12. Problem regions and FE meshes of electromagnetic fields.

skewed structures, which should be the main reason for such faults. In our opinion, this should be a very important and valuable discovery, which can provide important guidance for generator design and manufacturing to avoid such failures, and we have noticed that, before that, almost no similar public reports have been seen.

2) For the improvement scheme of such faults, the following three key requirements needed to be met. First, the loss and heat of the pole shoes should be effectively restrained. Second, the generator has to have a good no-load voltage waveform quality. Third, the improvement cost should be highly economic.

3) The second improvement scheme proposed in this paper met the above requirements. Therefore, satisfactory results were achieved after its implementation. Thus, the analysis and revelation of the fault mechanism in this paper are correct and reasonable. On this basis, the proposed improvement scheme is considered effective and reliable.

The research work of this paper can not only provide direct and effective guidance and reference for the treatment of this kind of fault and the design of new tubular hydro-generator, but also can help the generator manufacturer and hydropower plant avoid the economic loss caused by this kind of fault.

At the same time, it is worth mentioning that as the authors of this paper, we are undoubtedly very willing to publishfurther more quantitative analysis data in this paper. But such work can only be carried out after further agreement has been obtained from the generator manufacturer.In the future, we will further try to persuade generator manufacturers to allow us to publish more quantitative analysis data, and prepare a new paper for special discussion.

APPENDIX: THE ELECTROMAGNETIC FIELD MODEL

The influence of the skewed stator slot structure was analyzed to form a multi-slice electromagnetic field model of the generator.

According to the periodicity of the generator's magnetic field, a pair of poles was chosen as the electromagnetic field calculation region. Based on the stator slot skewed structural design, the generator was divided into twelve equal slices along the axial direction as shown in Fig. 12.

Considering the saturation of an iron core, the 3D boundary value problem of a nonlinear time-varying moving electromagnetic field was obtained as follows,

$$\begin{cases} \nabla \times (\nu \nabla \times \mathbf{A}) + \dfrac{1}{\rho}\left[\dfrac{\partial \mathbf{A}}{\partial t} - \mathbf{V} \times (\nabla \times \mathbf{A})\right] = \mathbf{J_s} \\ \mathbf{A}|_{Arc\_in} = \mathbf{A}|_{Arc\_out} = \mathbf{0} \\ \mathbf{A}|_{Ccylic\_boundary\_start} = \mathbf{A}|_{Ccylic\_boundary\_end} = \mathbf{0}, \end{cases} \tag{A1-1}$$

where $\mathbf{A}$ is the magnetic vector potential, $\mathbf{J_s}$ is the source current density, ν is the reluctivity, $\mathbf{V}$ is the velocity, and ρ is the resistivity.

For each slice, the current density and magnetic vector potential only have the axial z component, and the speed only has the circumferential x component. With the Coulomb norm $\nabla \cdot \mathbf{A} = 0$ and the boundary condition of the problem region, the 2D boundary value problem of the nonlinear time-varying moving electromagnetic was then obtained as follows,

$$\begin{cases} \dfrac{\partial}{\partial x}(\nu \dfrac{\partial A_{slz}}{\partial x}) + \dfrac{\partial}{\partial y}(\nu \dfrac{\partial A_{slz}}{\partial y}) = -J_{slz} + \dfrac{1}{\rho}\dfrac{\partial A_{slz}}{\partial t} + \dfrac{v_x}{\rho}\dfrac{\partial A_{slz}}{\partial x} \\ A_{slz}|_{arc\_in} = A_{slz}|_{Arc\_out} = 0 \\ A_{slz}|_{cylic\_boundary\_start} = A_{slz}|_{cylic\_boundary\_end}, \end{cases} \tag{A1-2}$$

where V_x is the circumferential component of the velocity, J_{slz} is the axial component of the source current density, and A_{slz} is the magnetic vector potential.

REFERENCES

[1] C.-Y. Li, "The application of bulb-type hydro-generator set at low head hydropower station," *Developing*, vol. 9, no. 9, pp. 145–146, Sep. 2006.
[2] S. Keller, M. Tu Xuan, J.-J. Simond, and A. Chwery, "Large low-speed hydro-generators—Unbalanced magnetic pulls and additional damper losses in eccentricity conditions," *IET Electr. Power Appl.*, vol. 21, no. 5, pp. 657–664, Sep. 2007.
[3] G. Baojun, L. Mingzhe, S. Yutian, L. Jinxiang, and H. Lijie, "Calculation of damper winding current for synchronous generators under asymmetric conditions," *Proc. Chin. Soc. Elect. Eng.*, vol. 33, no. 27, pp. 153–161, Sep. 2013.
[4] T. Pham, S. Salon, W. Akaishi, and M. DeBortoli, "Damper bar heating in hydro generators with fractional slot windings," in *Proc. IEEE Int. Electr. Mach. Drives Conf. (IEMDC)*, May 2017, pp. 1–8.
[5] K. Wen, L. Han, Z.-T. Zhou, Z.-N. Fan, Y. Liao, J. Wang, Z. Sun, B. Yao, and B.-D. Zhang, "3D electromagnetic-temperature field close-coupling calculation of losses and heat in the damper winding of a large tubular hydro-generator," *J. Electr. Eng. Technol.*, vol. 14, no. 3, pp. 1255–1268, May 2019.
[6] L. Cheng-Yuan, L. Yan-Ping, and C. Jing, "Calculation of rotor temperature field for huge hydro-generator," in *Proc. 6th Int. Forum Strategic Technol.*, Aug. 2011, pp. 524–528.
[7] S. Huiyong, Z. Guanghou, and H. Zhixin, "Calculation and analysis of electromagnetic field and temperature field of tubular turbine generator rotor," *Dongfang Electr. Rev.*, vol. 26, pp. 33–38, Jun. 2012.
[8] Z.-N. Fan, Y. Liao, L. Han, and L.-D. Xie, "No-load voltage waveform optimization and damper bars heat reduction of tubular hydrogenerator by different degree of adjusting damper bar pitch and skewing stator slot," *IEEE Trans. Energy Convers.*, vol. 28, no. 3, pp. 461–469, Sep. 2013.
[9] Z.-N. Fan, L. Han, Y. Liao, L.-D. Xie, K. Wen, J. Wang, X.-C. Dong, and B. Yao, "Effect of damper winding and stator slot skewing structure on no-load voltage waveform distortion and damper bar heat in large tubular hydro generator," *IEEE Access*, vol. 6, pp. 22281–22291, 2018.
[10] L. Weili, Z. Yu, and C. Yuhong, "Calculation and analysis of heat transfer coefficients and temperature fields of air-cooled large hydro-generator rotor excitation windings," *IEEE Trans. Energy Convers.*, vol. 26, no. 3, pp. 946–952, Sep. 2011.

[11] H.-X. Xia, Y.-Y. Yao, and G.-Z. Ni, "Analysis of ventilation fluid field and rotor temperature field of a generator," *Electr. Mach. Control*, vol. 11, no. 5, pp. 472–476, Oct. 2007.
[12] L. Weili, Z. Yu, and C. Yuhong, "Influence of rotation on rotor fluid and temperature distribution in a large air-cooled hydro-generator," *IEEE Trans. Energy Convers*, vol. 28, no. 1, pp. 117–124, Mar. 2013.
[13] L. Weili, L. Jinyang, and L. Dan, "Influence of variable cross-section rotor ventilation ditch on temperature field and fluid field of rotor for air-cooled hydro-generator," *J. Electr. Eng.*, vol. 32, pp. 42–49, Oct. 2017.
[14] S. Zhang, W. Li, J. Li, L. Wang, and X. Zhang, "Research on flow rule and thermal dissipation between the rotor poles of a fully air-cooled hydro-generator," *IEEE Trans. Ind. Electron.*, vol. 62, no. 6, pp. 3430–3437, Jun. 2015.
[15] W. Li, D. Li, J. Li, and X. Zhang, "Influence of rotor radial ventilation ducts number on temperature distribution of rotor excitation winding and fluid flow state between two poles of a fully air-cooled hydro-generator," *IEEE Trans. Ind. Electron.*, vol. 64, no. 5, pp. 3767–3775, May 2017.
[16] X. Haixia, L. Tao, and N. Guangzheng, "Analysis of flow field and rotor temperature field in ventilation system of generator," *J. Electr. Mach. Control*, vol. 11, no. 5, pp. 472–476, Sep. 2007.
[17] L.-X. Fu, *The Test Measures of Three Phases Synchronous Machine*, Standard GB/T 1029-2005, Standards Press of China, Beijing, 2013.
[18] B. Yan-Nian, *Design and Computation of Hydro-Generator*. Beijing, China: China Machine Press, 1982.

ZHI-TING ZHOU was born in Deyang, China, in 1999. She is currently pursuing the M.Sc. degree with Chongqing University. Her research interests include magnetic and thermal field calculation of generators, electrical machinery, and motor drives.

YONG YANG was born in Hubei, China, in 1982. He received the bachelor's degree in electrical machine from Chongqing University, Chongqing, China, in 2006. He is currently a Senior Engineer with Dongfang Electric Machinery Company Ltd. He is engaged in the electromagnetic analysis, calculation, and experimental research of electric machines.

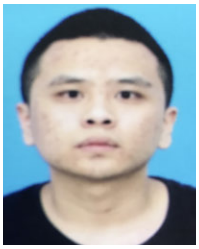

KE XIAO was born in Xuanhan, China, in 1992. He graduated from Xihua University. His research interests include magnetic and thermal field calculation of generators, electrical machinery, and motor drives.

ZHEN-NAN FAN was born in Longchang, China, in 1981. He received the Ph.D. degree in electrical engineering from Chongqing University, Chongqing, China, in 2013. He is currently an Associate Professor with Xihua University. His research interests include magnetic and thermal field calculation of generators, electrical machinery, and motor drives.

ZU-YING BIAN is currently pursuing the M.Sc. degree with Xihua University. His research interests include magnetic and thermal field calculation of generators, electrical machinery, and motor drives.

KUN WEN was born in Chongqing, China, in 1991. He received the M.Sc. degree from Xihua University, Chengdu, China, in 2019.

His research interests include magnetic and thermal field calculation of generators, electrical machinery, and motor drives.

JING-CAN LI was born in Yichang, China, in 1977. He received the Ph.D. degree in electrical engineering from Chongqing University, Chongqing, China, in 2011. He is currently a Lecturer with Chongqing University. His research interests include magnetic and thermal field calculation of generators, electrical machinery, motor drives, and control of electrical machines.

BING YAO was born in Sichuan, China, in 1981. He received the M.Sc. degree from Xihua University, Chengdu, China, in 2010. He is currently a Lecturer with Xihua University. His research interests include magnetic and thermal field calculation of generators, electrical machinery, and motor drives.